Deformation along an apparent seismic barrier: a palaeoseismological study along the North Anatolian Fault

Gero W. Michel(*) **and Christoph Janssen**
GeoForschungsZentrum Potsdam, Germany

Abstract
An overstep in the North Anatolian Fault, possibly acting as a seismic barrier, was investigated for its structural and palaeoseismological characteristics. Study interests were: i) to find overstep related spatial changes in deformation which would help assess the structure as a long term singularity in the fault; ii) to identify short term, event-triggered changes in structures where the major fault enters the overstep *i.e.*, in an area where seismogenic slip is impeded or even arrested; iii) to investigate whether or not the surface overstep is related to a seismic barrier, and iv) to discuss structures that might possibly be characteristic of barriers. In order to achieve this: a) largescale faults were mapped in the area, b) fault-slip data were measured in 56 outcrops along and within the overstep, and c) trenches were dug at the eastern rim of the overstep where recent earthquake structures had been reported. Derived long term stretching directions and ratios change significantly over the fault step and structures of recent major earthquakes suggest different deformation mechanisms for different events at the same location *e.g.* strike-slip, thrust and normal faulting.

Key words *geometric barrier – seismic barrier – palaeoseismology – earthquake geology – fault slip data – North Anatolian Fault*

1. Introduction

Palaeoseismological studies commonly include physical exploration, such as trenching to expose and permit microstratigraphic analyses and geomorphic techniques to consider palaeoearthquake magnitude, intensity, frequency, recency of last event, and probability of occurrence (Plafker and Rubin, 1967; Anderson, 1979; Slemmons and de Polo, 1986; Schwartz, 1987; Youd and Perkins, 1987; Pantosti and Yeats, 1993; Nikonov, 1995). The major aims of palaeoseismological studies are to contribute to: i) assessing hazards and risk of an area to mitigate future disasters; ii) understand earthquake related surface processes, and iii) find areas where major earthquakes clustered in the past and which might be suitable for monitoring precursory effects. Palaeoseismological studies concentrate largely on stratigraphy and surface structures but additional approaches are necessary to enhance knowledge on the long term distribution of earthquakes or slip rates or the mechanisms and processes at depth that lead to the effects studied at the surface. Examples are: studies of palaeoseismicity relicts in crystalline rocks or slickenside surfaces (Mawer and Williams, 1985; Power and Tullis, 1989) or the investigation of palaeofluids related to seismogenic faulting (*e.g.* Parry and Bruhn, 1990) among others. Our contribution attempts to incorporate fault slip investigations into palaeoseismological approaches to relate a major geometric singularity in the North Anatolian Fault to a possible seismic barrier.

(*) e-mail: fault @ gfz.potsdam.de

Irregularities along major faults such as bends or oversteps, hereinafter referred to as geometric barriers, are often related to seismic barriers along which seismogenic slip is impeded or even arrested (Das and Aki, 1977; King and Yielding, 1983; King, 1986). Localized deformation changes into distributed deformation along minor transfer faults connecting the overstepping major fault segments in an area where high initial stresses cannot be reached (Das and Aki, 1977; Aki, 1979). Aftershocks and afterslip often concentrate within these areas (Sibson, 1985). Both stresses and strains are assumed to redistribute while deformation enters the barrier (see also Rodgers, 1980; Mann *et al.*, 1983; Xiahaon, 1983; Hempton and Neher, 1986; Cundall, 1990; Westerway, 1994). Seismic barriers are critical in earthquake mechanics and initiation, taking into account that termination of one event may set up the initiation environment for future events. Reports showing that major earthquakes often initiate in the vicinity of barriers are abundant (King and Nabelek, 1985) and the area around barriers might hence be worth monitoring for precursory effects. Barriers are assumed to govern segment rupturing in «characteristic earthquakes» (Schwartz and Coppersmith, 1984) and geometric barriers are often used to approximately define fault segments (*e.g.*, Bellier and Sebrier, 1995). However, it is critical to identify seismic barriers using singularities in the surface trace of a fault if no additional (*e.g.*, seismic) information is available.

Our investigation is part of a joint Turkish-German earthquake research project that investigates the Western North-Anatolian Fault and the READINESS Project (Real Time Data Investigation Network in Earth Science S), which studies the interaction of major faults in the Eastern Mediterranean and adjacent areas. Joint Turkish-German Project activities cluster in an area around a 1.5 km rightstep in the active North Anatolian Fault near Taskesti (31°01′E, 40°34′N) that marks a significant change in the direction of the fault zone (see below). The area was affected by recent major earthquakes and related ruptures terminated or nucleated within the overstep (see below). Background seismicity is currently low compared to the adjacent areas. Unfortunately no seismic profile of the study area is yet available to help interpret the deeper structure of the fault. We therefore had to rely on the remote and field investigation of surface deformation and results from the investigation of trenches. Aims at this site were to: i) identify the overstep as a long term structure which makes its penetration to the brittle-plastic transition most probable; ii) find either spatial or temporal changes in earthquake related deformation where ruptures enter the overstep, and iii) discuss structures that might be characteristically found along barriers. In order to do this, we investigated macroscale and mesoscale faults and carried out palaeoseismological studies, trenched for recent fault scarps, dated displaced sediments, and derived apparent (*i.e.*, near surface) rupture mechanisms using palinspastic reconstructions and by inverting movement patterns preserved within striations along displaced pebbles.

2. Study area and recent major earthquakes

Our study area covers a western section of the dextral North Anatolian major fault. The fault depicts the northern border of the Anatolian block extruding westward relative to Eurasia (fig. 1). The fault extends from Karliova in the East of Turkey over more than 1200 km to the Gulf of Saros and Edremit and apparently reaches further to the West in possibly two main traces to the Islands of Skiatos and Euböa (two Greek islands NE of Athens, Barakou *et al.*, 1994) where its further trace becomes obscured. We chose an area of detailed investigation along the major fault zone near Taskesti (shown in fig. 3d) where: a) the fault zone trend changes clockwise from 75° in the East to 110° in the West (fig. 2; Michel, 1994); b) the major fault steps approximately 1.5 km to the right displaying an area of low topography and abundant surface depressions (fig. 2), and c) crystalline basement of predominantly amphibolithic rocks to the North of the fault face Mesozoic calcareous rocks to the South. Within the last 52 years three major earthquakes shook the area exhibiting one epicenter

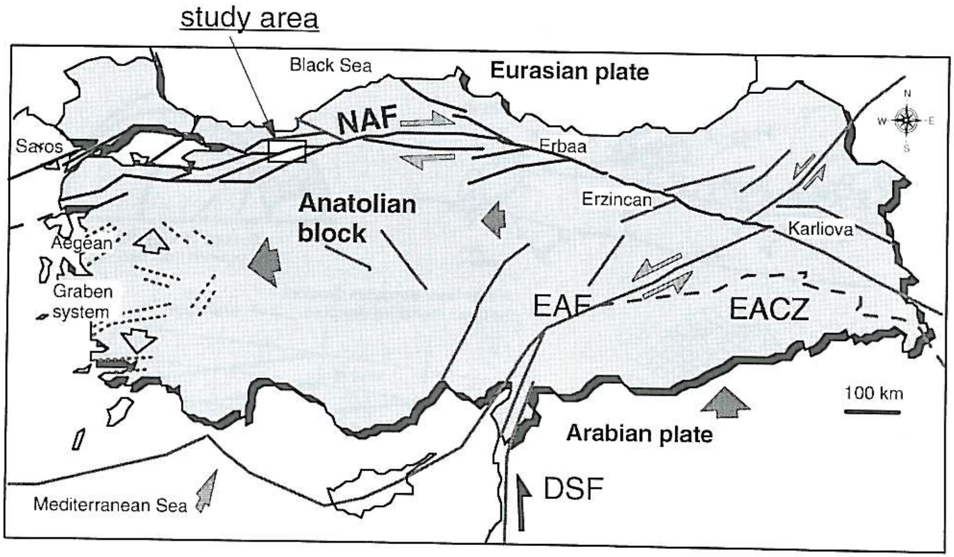

Fig. 1. The North Anatolian Fault represents the northern border of the Anatolian block which extrudes westward relative to Eurasia. Possible reasons for this movement are: 1) convergence, areal contraction and subsequent uplift in eastern Turkey, which force *i.e.*, push the Anatolian block to the west and 2) roll back of the subducting plate within the Aegean that possibly pulls the Anatolian block westwards. NAF = North Anatolian Fault; EAF = East Anatolian Fault; DSF = Dead Sea Fault; EACF = East Anatolian Convergence Zone.

Fig. 2. View of the overstep (Landsat TM scene).

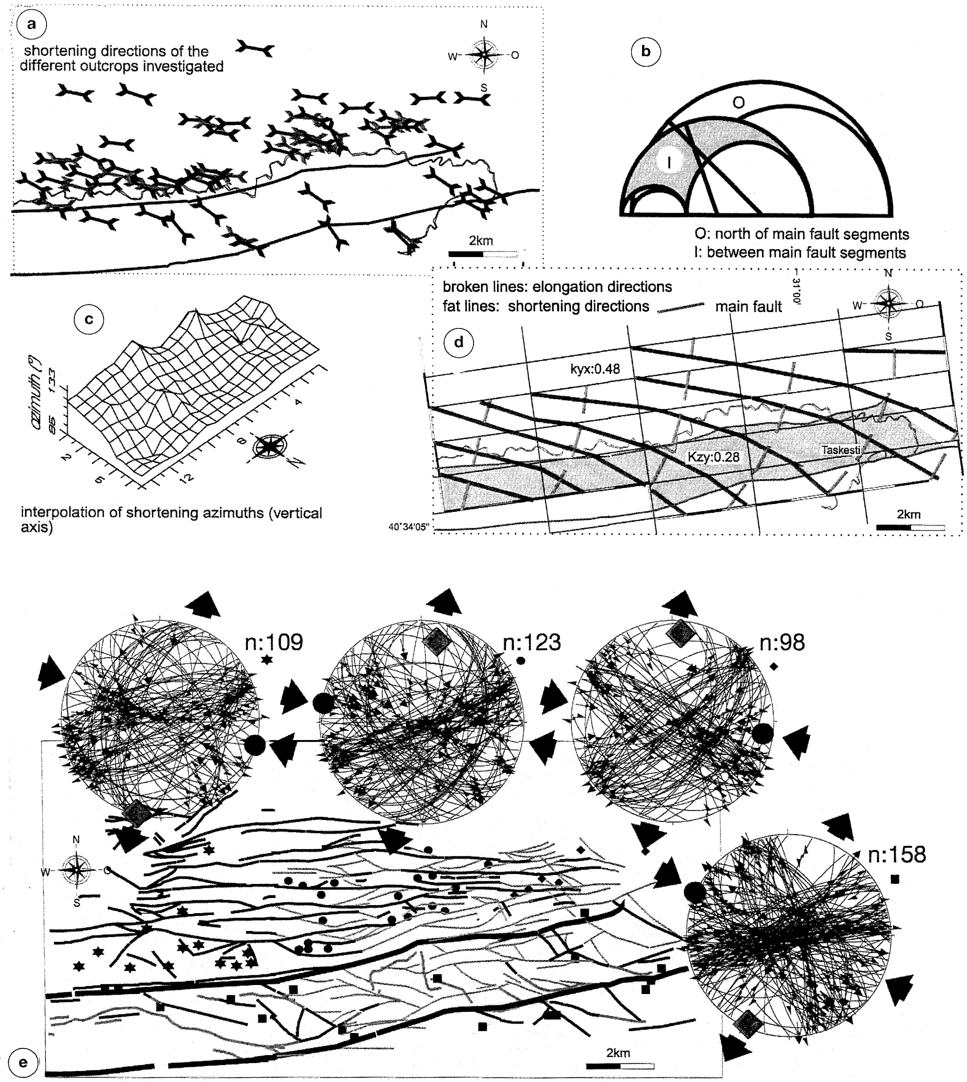

Fig. 3a-e. a) Major fault and shortening directions derived using fault-slip data. Each arrow in the map in (a) represents an infinitesimal shortening direction derived for one outcrop population of fresh faults and the youngest deformation found in the study area. The different arrow grey shades aim to improve visual discrimination between arrows. Figure 3e represents equal area projections of the fault slip data. Black squares and circles in the projections represent the cumulative directions of infinitesimal extension and shortening (minimum stretching), respectively. Interpolated shortening and extension directions indicate a spatial change in trend clockwise over the overstep (b,c,d). Numbers in (d) represent the computed composite axes ratio solutions for the area north of the overstep and within the overstep, respectively. The vertical axis in the 3D figure (c) represents the derived shortening azimuths within an interpolation network denser than in (d). Mohr half circles in (b) illustrate the different derived stress ratios calculated using: 1) computed stretches; 2) standard poisson ratios p and E-moduli e (amphibolite, area O, p: 120 GPa and e: 0.23 and limestone, area i, p: 0.3, e: 70 GPa.), and 3) zero dilation. E-W to ENE-WSW trending lines in (a) and (d) indicate the main fault traces.

at the overstep and two adjacent to it. The surface ruptures of the 1957 M_s 7 earthquake nucleated approximately 25 km to the East of the study area following and then terminating along the fault strand that bounds the overstep to the south (Ambraseys, 1970, local witnesses). A horizontal displacement of 1.6 m and a rupture length of about 60 km were inferred (Ezen, 1981). In contrast, the epicenter of the major subevent of the complex 1967 M_s 7.1 earthquake was located along the northern strand of the fault roughly opposite the 1957 rupture termination area (westernmost area in fig. 3a,d). The 1967 ruptures were mapped carefully by Ambraseys *et al.* (1968) and suggest that slip was distributed along various splays and followed additional transfer faults within the overstep (fig. 4). The maximum horizontal displacement reached 1.9 m but vertical slip dominated along faults within the overstep. Different subevents (6-7) were identified using teleseismic body waves for the 1967 earthquake (Stewart and Kanamori, 1982; Pinar *et al.*, 1996). Dextral strike-slip faulting was found to be dominant, however, two minor subevents showed normal faulting mechanisms, one a reverse faulting mechanism. A further major earthquake affected the area in 1944 (M_s: 7.2), nucleating about 100 km further east. The rupture possibly stopped within the eastern part of the investigation area (Barka and Kadinsky-Cade, 1988), and was followed by two intermediate shocks located adjacent to the overstep (Alsan *et al.*, 1975).

3. Fault and structural investigations

Our fault studies covered different scales in order to relate: a) mesoscally derived stretching directions to changes in macroscale fault distributions; b) describe deformation-related mechanisms, and c) find indications for co- and/or aseismic movements on the mesoscale faults. The latter task is not yet unequivocally possible and only a short portion of the mea-

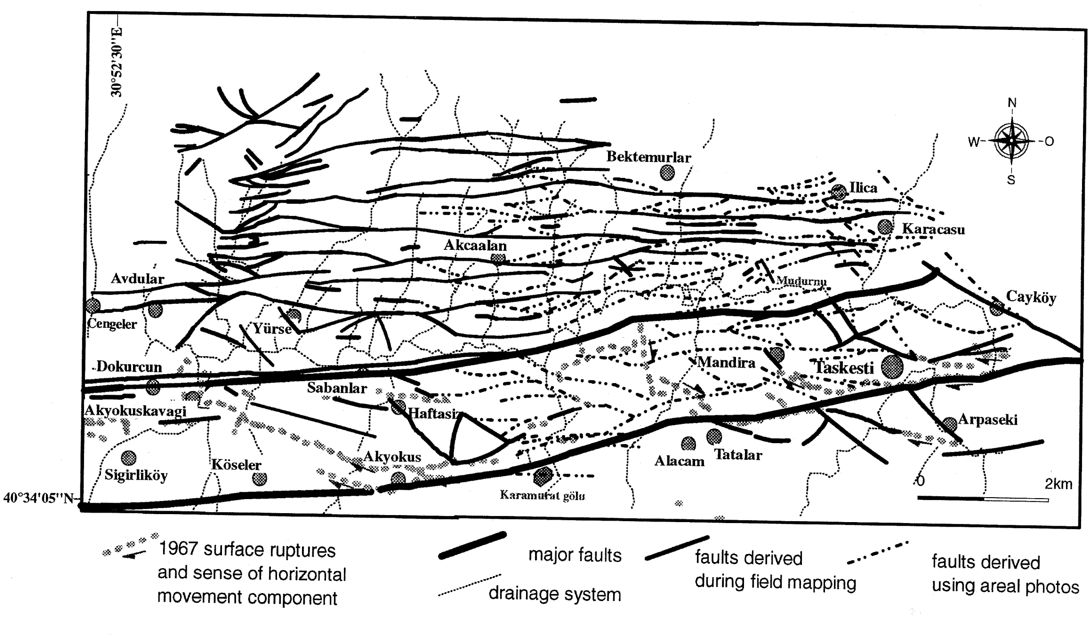

Fig. 4. Surface ruptures of the 1967 Mudurnu earthquake are distributed within the overstep (data after Ambraseys *et al.*, 1968).

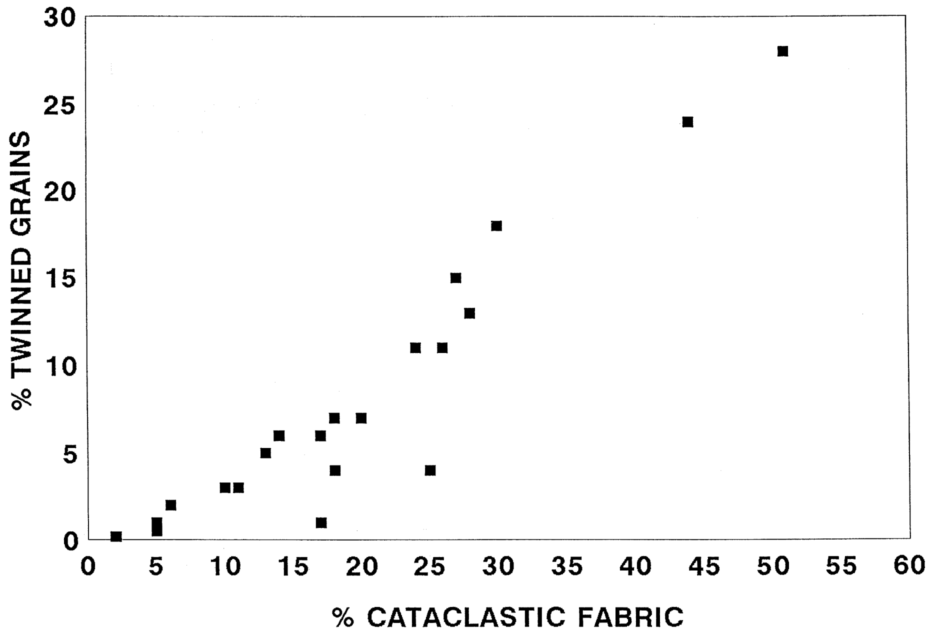

Fig. 5. Twinned grains represent crystalplastic deformation which is opposed to cataclastic event-triggered deformation accomodated by movements along faults, diminishing of grains, and rupturing of fractures. Each of the printed dots represent one thin section analysis. Point counting of 500 points was performed along 5 traverses for each thin section. The roughly linear correlation of crystalplastic and cataclastic fabric suggests, that they occurred quasi-penecontemporaneously, *i.e.*, possibly represent seismic cycles. Twinned grains may hence represent deformation within the pre-, post- and interseismic period whereas the cataclastic fabric might originate preferentially during co-seismic movements.

sured mesocale faults were studied microscopically. Future investigations are necessary to help assess structures of different scales as clearly coseismic. Our microscopic observations were concentrated on calcareous rocks of lower Tertiary and younger ages located within or adjacent to the exposed core of the major fault, where deformation was dominated by North-Anatolian Fault activities. The observations revealed that fracturing, twinning and pressure solution processes led to comminution of the host rock and the development of protocataclasites to ultracataclasites (Sibson, 1977). They are composed of subrounded to subangular carbonate fragments embedded in a fine grained matrix. Pressure solution seems mutually cross-cut cataclastic microstructures suggesting that both deformation mechanisms occurred concurrently. Cataclastic microstructures are more abundant than relicts of twinning but relative numbers correlate roughly linearly (fig. 5). Progressive brittle failure led to local development of fault breccias. They depict a crude foliation defined by preferred orientation of fractures and anisotropically oriented fragments. The fragments show no or only little evidence of frictional attrition. Most of the fragment boundaries match those of adjacent clasts forming an exploded jigsaw texture and fractures are all open.

Figure 3e includes major and minor faults which we mapped both in the field and using aerial photos. The rose diagrams in fig. 6a-c represent the cumulative distribution of the fault trends (field mapping) as well as lineaments (airphotos) north of the overstep (a) and

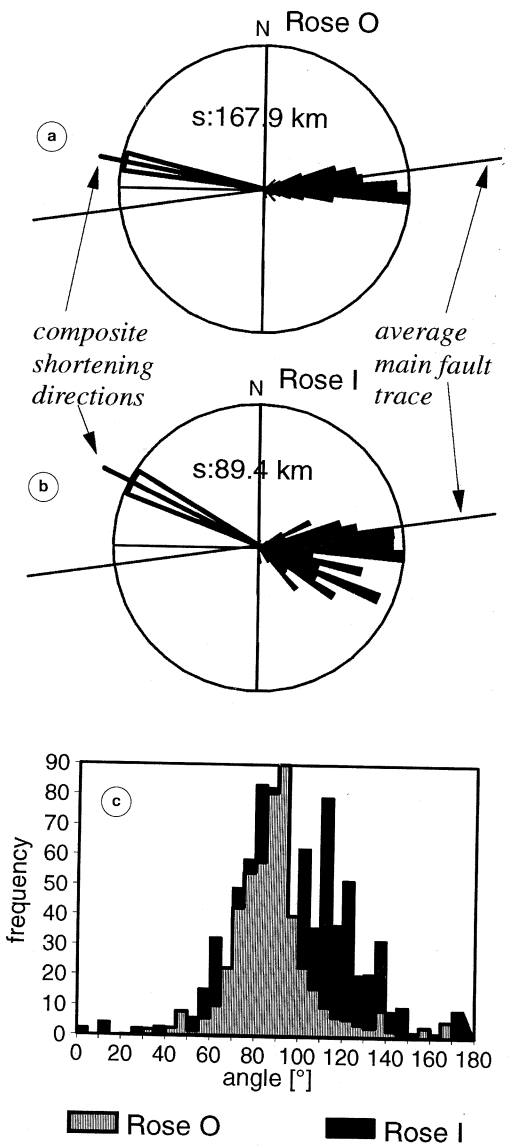

Fig. 6a-c. Rose and block diagrams showing the distributions of fault directions weighted with their mapped lengths. Within the overstep (i in figure b and c), we found NW-SE patterns of faults, in addition to patterns similar to those we found outside the overstep (o in figure a and c). We suggest that the first represent transfer and/or splay faults. Composite shortening directions are derived using the measured fault slip data shown in figure 3e. Cones represent 95% confidence limits.

within the overstep (b). Trends were weighted using the relative length of straight (deviation: ± 1°, 1:20000) segments. The NW-SE maximum in the rose diagram (b) roughly coincides with the splay and transfer faults mapped by Ambraseys. Infinitesimal shortening directions were derived using data from mesoscale faults with associated striations (Allmendinger, 1989; Michel, 1993). Only those faults that depict a number of similar second order features (Petit, 1987) indicating a clear sense of slip were used. Where possible (within the overstep as well as within several small Holocene deposits adjacent to the overstep), fault slip analyses were restricted to Quaternary deposits. Additional investigations in older sediments and basement rocks were carried out along the overstep in order to obtain subregional deformation trends. Data of the latter were pre-investigated in the field for temporal successions in faulting and only the youngest movements found in each measured outcrop were used for this study (Michel *et al.*, 1995). They were all found along macroscopically unweathered fault planes along which fine cataclastic material was preserved. We hence suggest that the derived shortening directions (see below) represent the recent deformation (Michel *et al.*, 1995). In order to approximate principal directions of infinitesimal strain using the measured fault populations, we used a procedure that optimizes and then describes clusters of shortening and extension directions derived for each plane using Bingham distributions. Derived directions are comparable to seismological P- and T-directions and are derived taking into account a best fitting Coulomb friction behaviour (Michel, 1993). We analysed three dimensional distributions of derived infinitesimal extension and shortening directions and, because most of the derived directions are subhorizontal (± 10°), concentrated on the shortening azimuths (fig. 3a). Results suggest that shortening directions bend clockwise over the overstep (fig. 3a,c,d for explanation see figure captions). Derived shortening trajectory trend between 96° (N over E) in the N and 133° in the S. 95% confidence limits, derived using Bingham distributions for data of the different outcrops, range between a few and 20° and are well below this overall change in trend. In order not to lengthen this paper we decided to leave out the statistics of the single outcrops, they can be ordered from the authors. Strike-slip faulting dominates in the deformation patterns in the area north of the overstep, whereas strike-slip, oblique slip, and normal faulting are abundant within the overstep. Michel (1993) showed that ratios of infinitesimal stretching for a population of measured faults may be approximated using the distribution of shortening and/or extension directions for each fault. Two dimensional deformation requires that both directions cluster in a population, whereas if extension directions describe a girdle and shortening directions a cluster, flattening deformation is approximated. The opposite suggests constrictional deformation. We found flattening deformation outside and constrictional deformation inside the overstep. Ratios are drawn in fig. 3d. Relative stress ratios were approximated using standard stress-strain relations for the different lithologies measured (fig. 3b, for explanation see figure caption). They suggest that faulting occurred under equal (relative) shear and normal stresses, whereas the (relative) maximum stress, mean stress, and the stress parallel to the fault segments were lower within the overstep. Large block rotations were not detected in the area using palaeomagnetic investigations (Michel *et al.*, 1995). However, associated deviation limits reach 30° and a change in directions due to the congruent rotation of several blocks cannot be excluded.

Mesoscale faults showing the derived change in direction are abundant within the studied area and representative for the youngest phase in brittle deformation derived (Michel *et al.*, 1995). Taking into account that the older deformation system has an approximate Miocene to lower Pliocene age (Michel *et al.*, 1995), the deformation accomodated by the faults presented herein represent a time span of millions rather than thousands of years. The presented fault slip solutions are composite solutions and possible short time changes or differences in deformation triggered by single events are not discerned.

4. Investigation of major palaeo-earthquakes

A variety of palaeoseismological studies infer that faults or fault segments rupture in series of characteristic earthquakes, each identical in size and slip distribution. This characteristic earthquake model requires that seismogenic slip varies along the fault and vanishes when approaching the ends of the fault segments. The seismogenic slip rate along the fault is hence assumed to vary too (Schwartz and Coppersmith, 1984). Consequently many palaeoseismological studies concentrate on the inner part of fault segments where deformation and slip rates are assumed to be large. Little has yet been done to study local events triggered changes in deformation in areas where rupture processes are assumed to vary and seismogenic slip is assumed to change and/or vanish, *e.g.* near barriers. In order to investigate recent earthquake related faulting, we trenched East of but adjacent to the overstep near Taskesti (fig. 7), where we assumed that movements might change from localized to distributed. Four trenches were dug adjacent to each other, three to investigate earthquake near-surface structures and one for the local stratigraphic succession. The succession starts with a pebbly layer found in the bottom of all trenches. It underlies sand-silt and clay layers of varying thicknesses. Two clay layers that carry abundant charcoal, one adjacent to the pebbly layer and one below the eroded surface, were dated using the ^{14}C method. Calibrated ages are 4167 ± 168 and 4120 ± 125 years (B.C.), for the two layers, respectively. No paleosol horizons were found and the trenched sections were cut by a landslide. Figure 8a shows a western section of the westernmost trench. The trenched apparent vertical displacement of 1.4 m of the pebbly layer is accompanied by a few additional smaller ruptures. Similar structures were found in a second trench 150 m to the East of the first one. After leaving the pebbly layer, the ruptures splay and the total displacement is distributed with only part of the displacement being localized on the different splays (see numbers on fig. 8a). Displacements along the splays die out within a few decimeters. What is left is a bend

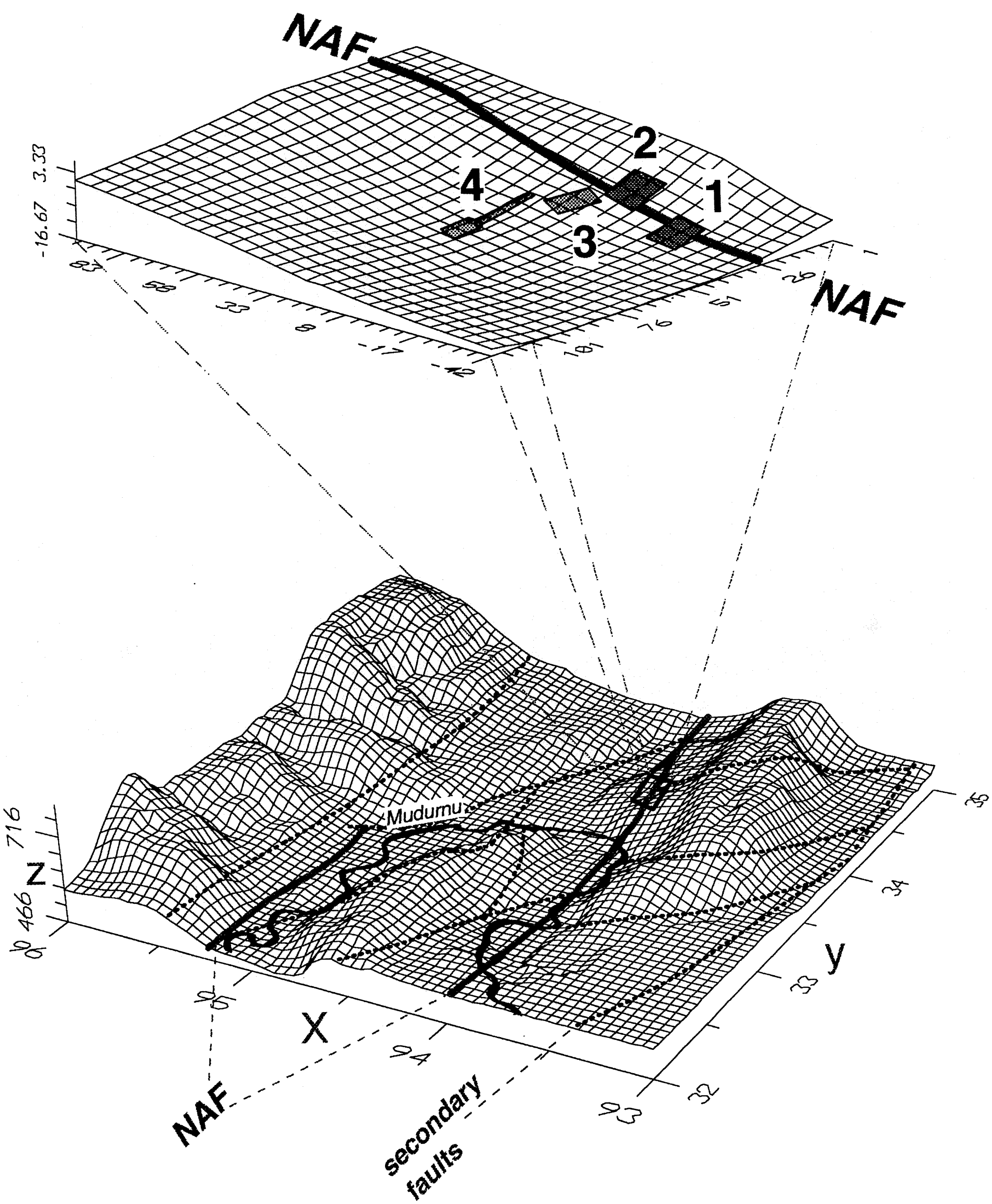

Fig. 7. Locations of the different trenches with respect to the major fault and topography. NAF = North Anatolian major Fault; *x* and *y* axes denote latitudes and longitudes (UTM), *z* the altitude [m o.N.N.]; numbers 1-4 denote the different trenches: figs. 8a,b and 9 show parts of trench 1; trench 2 depicted structures similar to those found in trench 1 (see text), fig. 11 shows the eastern wall of trench 3, trench 4 was dug to evaluate the stratigraphy.

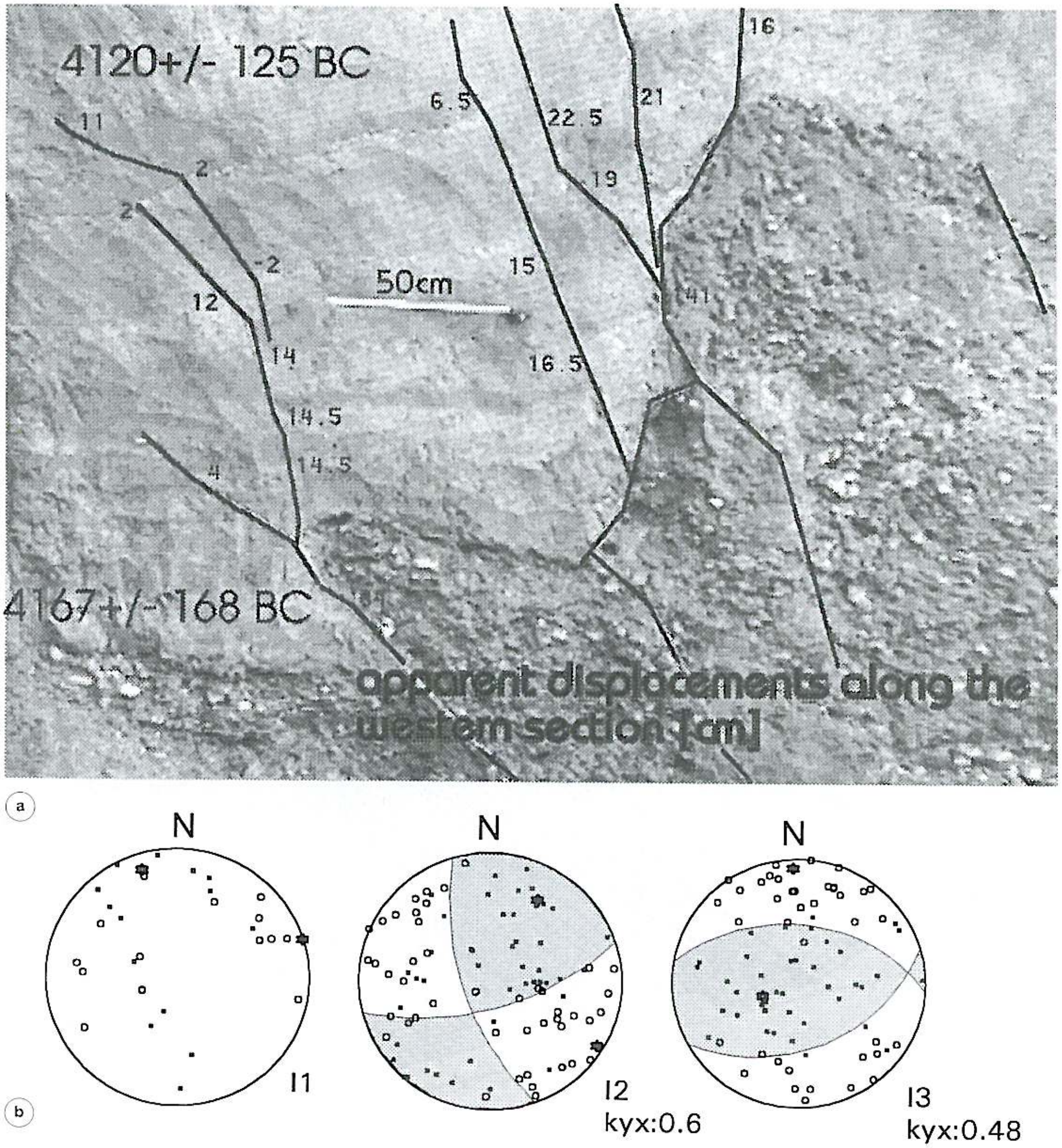

Fig. 8a,b. View of the western wall of the westernmost trench. Numbers in the upper part of the figure are apparent (2D) displacements of exposed layers. The equal area projections in the lower part of the figure show shortening and elongation directions derived using successions of stria lines on the pebbles. They were derived assuming that deformation might be explained by simple shear along each tangential plane and hence with shortening and extension directions in an angular distance of 45° to the tangential planes (see text). Errors induced by this assumption are low in most cases (Célérier, 1988). Open circles represent shortening directions, dots represent extension directions. The projections depict a succession in deformation from diffuse (left, I1) over strike-slip faulting (middle, I2) to reverse faulting (right, I3). The derived high ky*x*-ratios suggest that the pebbles displayed minor rotation and/or deformation was three dimensional.

with an apparent amplitude of 2.5 m. Because displaced paleosol horizons were lacking, we were not able to unequivocally distinguish between events. In order to derive the slip directions represented by the apparent vertical displacements, we sampled a variety of oriented pebbles along the main ruptures within these two trenches and investigated the preserved striation directions on them in the laboratory. Measured stria lines are almost straight suggesting that the pebbles did not or only slightly rotated during faulting. Cross-cutting relationships of the stria lines suggest that the structures represent at least two (possibly three) events of different attitudes *i.e.*, of different slip directions.

An event herein is not necessarily related to a major earthquake and may also represent a creep event or several small earthquakes within a sequence showing similar mechanisms. Except for eight of the measured stria lines for the last event (see below) all stria lines of the youngest event displaced older events and the relative age of the last two events is well constrained. Figure 8b shows infinitesimal stretching directions derived creating planes tangential to average major stria on the pebbles and computing shortening and extension directions in planes perpendicular to the tangential planes through the striation directions (see also P- and T-directions of fault plane solutions). Results suggest that, after a possible first event with diffuse uncertain character, a second event accomodated dextral strike-slip deformation along the E-W trending main fault. This is in contrast to a third event that created N-S thrust faulting. ky$x$-ratios represent the distributions of the extension axes, *i.e.*, the associated ratios of the computed intermediate to largest eigenvalues (Michel *et al.*, 1995). The high numbers reflect the wide scattering of the data suggesting minor rotation of pebbles and/or three di-

Fig. 9. A graben structure found in the westernmost trench, 3 m north of the structure shown in fig. 8a,b.

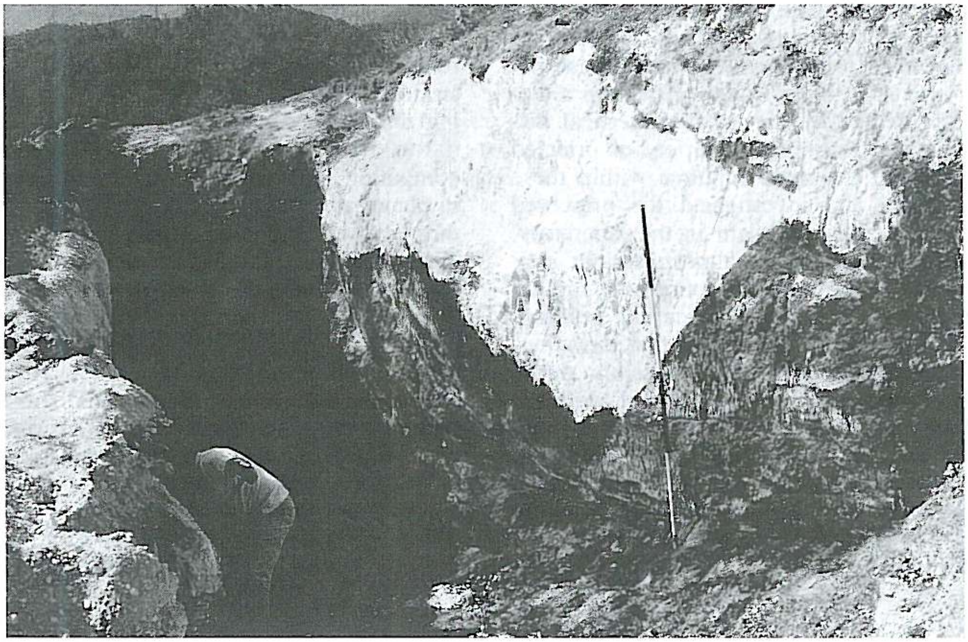

Fig. 10. Trenched normal faulting within the overstep.

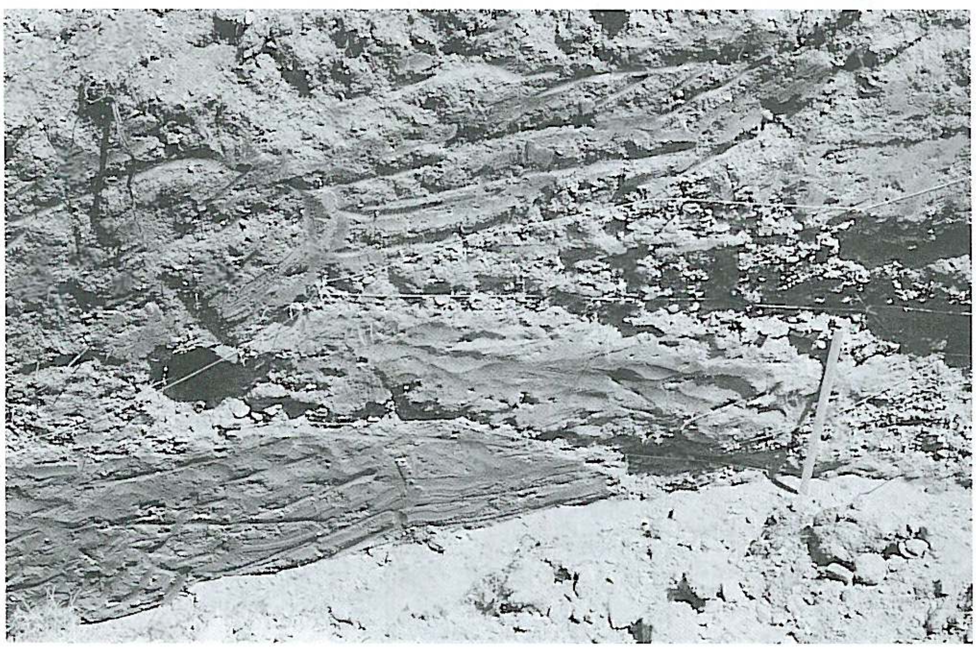

Fig. 11. View on the eastern wall of trench 3 (fig. 7). Structures suggest reverse faulting.

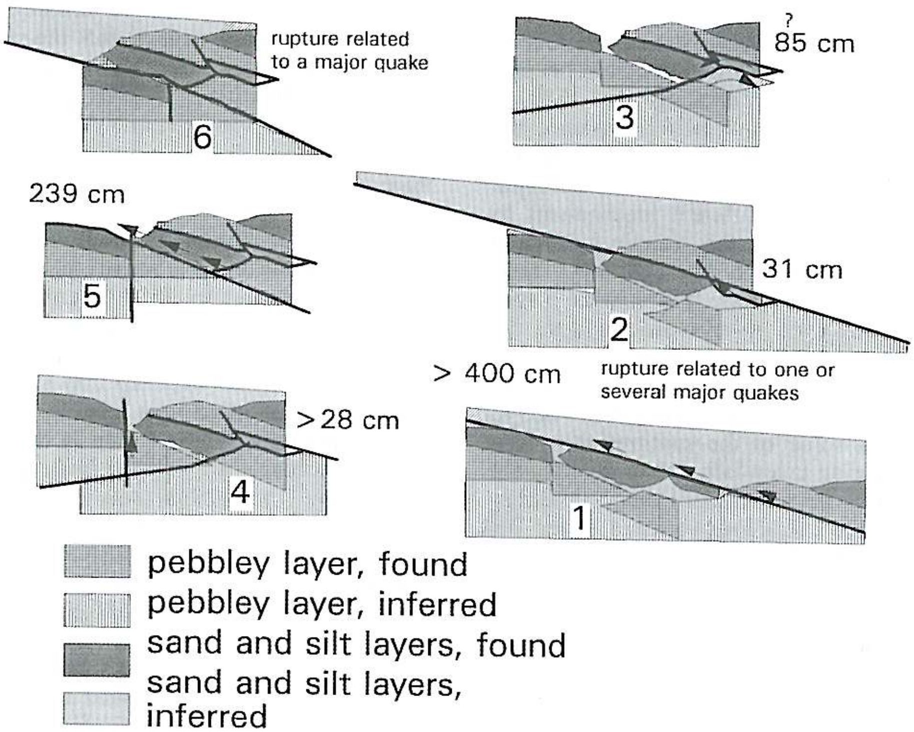

Fig. 12. A possible reconstruction of the structures found in trench 3 shown in fig. 11. Numbers from 1 to 6, represent steps in evolution of the structure, with 1 representing the oldest and 6 the most recent *i.e.*, youngest step, respectively.

mensional deformation conditions. North of the described structures in the first easternmost trench, a graben-like structure was observed (fig. 9) suggesting N-S extension. A variety of structures indicating normal fault were found within the overstep fig. 10. Figure 11 shows a third trench 400 m to the East and 120 m North of the second one. The pebbly layer, which originally was located below the mapped silt- and clay layers, was apparently thrust over the latter suggesting slip of more than 4 m. Figure 12 exhibits a possible reconstruction of the detected structures. This trench depicted at least two events that apparently accomodated N-S convergence. The top of each trench was cut by a landslide and the ^{14}C ages mentioned above give only a lower possible age of deformation of the movements mapped.

5. Results and conclusions

The recent faulting and earthquake ruptures studied suggest that an overstep in the western dextral North-Anatolian major fault near Taskesti depicts the end of a segment and possibly acts as a seismic barrier, where seismic slip impedes or even arrests, or ruptures nucleate. We investigated the area for possible long term spatial and short term «event triggered» changes in deformation using: a) structural studies of mesoscale fault-slip data distributed within 56 outcrops over the area; b) microscale, and c) trench investigations. Microscale patterns suggest that deformation was accommodated by both long term crystalplastic deformation and apparent short term rupturing. An almost linear correlation of mechanism-related structure distributions suggest that areas that suffered high crystalplastic deformation also suffered high intensities in brittle faulting. Because structures indicating the different mechanisms crosscut mutually we assume that both mechanisms occurred concurrently *i.e.*, within the same overall deformation and depth. We suggest that the different mechanisms reflect different steps in the seismic cycle with co-seismic sudden rupturing and pre-, inter-, and post-seimic longterm viscoplastic straining. However, even if structures indicate different mechanisms, unequivocally assessing whether structures originated during long term creep, creep events, or co-seismically is not yet possible and some of the ruptures may have nucleated during creep rather than seismic slip. We restricted our preliminary micro-investigations to similar calcareous rocks of lower Tertiary and younger age within outcrops at the major fault core. We were not able to detect lateral changes in mechanism-distribution-ratios within and adjacent to the overstep within these limited numbers of outcrops.

Macro and meso deformation structures indicate a long term change in deformation along and over the fault step. Derived infinitesimal shortening directions rotate clockwise over the step and deformation changes from strike-slip outside the overstep to oblique normal faulting within it. Derived relative stresses are different so that relative mean and maximum stresses are lower within the overstep. We assume that this change in stress reflects a weakening of the intrinsic material within the apparent barrier in addition to the noted change in lithologies (Cundall, 1990). As opposed to this apparent characteristic long term spatial change in deformation and stress, structures which are assumed to represent major events east of the overstep are non-characteristic for a dextral transcurrent fault and show multifold deformation including normal, strike-slip, and thrust faulting. According to the ^{14}C ages of displaced sediments the structures found are younger than 4120 ± 125 B.C. In addition to the trench investigation of structures, we analyzed distributions of stria lines along pebbles sampled along the exposed faults; an effort that might help to differentiate events where displaced paleosol horizons are missing. Crosscutting relationships suggest that the stria lines were products of different events showing different slip directions. Derived differences in mechanisms are too high to be the result of local undulations in the almost straight fault trace east of the overstep (Sonder, 1990) and are related to the influence of the latter. We hence interpret the derived multifold deformation as representing a complex change in deformation adjacent to an overstep, within an area where seismic slip is impeded or arrested: different amounts of co-seismically overshooting slip entering the overstep may shift the position of the trenched area relative to a single event slip-termination resulting in different local slip mechanisms. A near, high gradient in diminishing horizontal seismic slip may change the local apparent mechanism from strike-slip to transpression displaying contraction and uplift (Bilham and King, 1989). Structures indicating local, roughly pure strike-slip movements suggest, that associated seismic slip did not impede or arrest in the vicinity of the trenched area. They moved further, possibly concentrating on one of the overstep bounding major fault segments. Transtensional movements may occur if seismic slip nucleates west of the overstep, propagate with dimished velocity through the overstep, and reaches the trenched area with increasing velocity. We suggest that the trenched graben structure is related to the latter mechanism. We cannot exclude that our «events» are in part aseismic and some of the striations along the investigated pebbles might represent creep events or long term creep. Inverted patterns of teleseismic body waves of the complex 1967 earthquake (Pinar *et al.*, 1996) showed subevents with mechanisms different from strike-slip faulting east and west of the overstep. A subevent showing reverse faulting occurred East of the overstep and hence correlates with the abundant reverse faulting that we found within our trenches. We conclude that our structural and palaeoseismological investigations favor the overstep in representing a longterm seismic barrier. However, we should keep in mind, that seismic slip changes its attitude while propagating to the free surface, where palaeoseismological effects similar to those described above may be induced. Additional work is necessary to define spatial changes in deformation or successions of surface structures as clear indicators for local or regional seismic barriers.

Acknowledgements

We thank Sinan Gencoglu and his crew for their support. Especially we would like to gratefully acknowledge Jochen Zschau, without him neither the project nor our studies would have been possible.

REFERENCES

AKI, K. (1979): Characterization of barriers on an earthquake fault., *J. Geophys. Res.*, **84**, 6130-6147.

ALLMENDINGER, R.W. (1989): Notes on fault slip analysis, *Short course on the «Quantitative Interpretation of Joints and Faults»*, Department of Geological Sciences Cornell University Ithaca, New York.

ALSAN, E., L. TEZUCAN and M. BATH (1975): *An Earthquake Catalogue for Turkey for the Interval, 1913-1970*, Kandili Observatory Seismological Dept., Cengelköy-Istanbul, and Seismological Observatory Uppsala, Sweden, Rep., No. 7-75.

AMBRASEYS, N.N. (1970): Some characteristic features of the Anatolian Fault Zone, Tectonophysics, **9**, 143-165.

AMBRASEYS, N.N., A. ZATOPEK, M. TASDEMIROGLU and A. AYTUN (1968): The West Anatolian earthquake of 22 July 1967, *UNESCO Publ. Ser.*, Paris, p. 622.

ANDERSON, J.G. (1979): Estimating seismicity from geological structures for seismic-risk studies, *Bull. Seism. Soc. Am.*, **69**, 163-168.

BARAKOU, TH., N. DELIBASIS, M. ZIAZIA, G. KARANTONIS, N. VOULGARIS, H. BERCKHEMER, B. BAIER, B. KARAKOSTAS and D. PANAGIOTOPOULOS (1994): Seismicity and seismotectonics of the North Aegean Sea. Preliminary results from the North Aegean Sea Network (NASN). ESC, abstracts, 30, *J. Struct. Geol.*, **11**, 275-283.

BARKA, A.A. and K. KADINSKY-CADE (1988): Strike-slip fault geometry in Turkey and its influence on earthquake activity, *Tectonics*, **7**, 663-684.

BELLIER, O. and M. SEBRIER (1995): Long-term fault slip rate and arc domain deformation in Sumatra (Indonesia), *Terra abstracts*, **7**, 37.

BILHAM, R. and G. KING (1989): The morphology of strike-slip faults: examples from the San Andreas Fault, California, *J. Geophys. Res.*, **94**, 10204-10216.

CÉLÉRIER, B. (1988): How much does slip on a reactivated fault plane constrain the stress tensor? *Tectonics*, **7**, 1257-1278.

CUNDALL, P.A. (1990): Numerical modelling of jointed and faulted rock, in *Mechanics of Jointed and Faulted Rock* edited by H.P. ROSSMANITH (A.A. Balkema, Rotterdam, Brookfield), 11-18.

DAS, S. and K. AKI (1977): Fault planes with barriers: a versatile earthquake model, *J. Geophys. Res.*, **82**, 5658-5670.

EZEN, U. (1981): Earthquake-soucre parameters related to magnitude along the North Anatolian fault zone, *Bull. IISEE*, **19**, 33-55.

HEMPTON, M.R. and K. NEHER (1986): Experimental fracture, strain and subsidence patterns over en échelon strike-slip faults: implications for the structural evolution of pull-apart basins, *J. Struct. Geol.*, **8**, 597-605.

KING, G.C.P. (1986): Speculations on the geometry of the initiation and termination process of earthquake rupture and its relation to morphology and geological structures, *PAGEOPH*, **124**, 567-584.

KING, G.C.P. and G. YIELDING (1983): The evolution of a thrust fault system: processes of rupture initiation, propagation and termination in the 1980 El Asnam (Algeria) earthquake, *Geophys. J. R. Astron. Soc.*, **77**, 915-933.

KING, G.C.P. and J. NABELEK (1985): The role of bends in faults in the initiation and termination of earthquake rupture, *Science*, **228**, 984-987.

MANN, P., M.R. HEMPTON, D.C. BRADLEY and K. BURKE (1983): Development of pull-apart basins, *J. Geology*, **91**, 529-554.

MAWER C.K. and P.F. WILLIAMS (1985): Crystalline rocks as possible palaeoseismicity indicators, *Geology*, **13**, 100-102.

MICHEL, G.W. (1993): Modeling fault-slip data sets: a key for approximating stretching ratios? *Z. dt. Geol. Ges.*, **144**, 150-158.

MICHEL, G.W. (1994): Neo-kinematics along the North-Anatolian Fault, Turkey, *Tübinger Geol. Abh.*, **16**, p. 249.

MICHEL, G.W., M. WALDHOER, J. NEUGEBAUER and E. APPEL (1995): Sequential rotation of stretching axes and block rotations; a structural and palaeomagnetic study along the North-Anatolian Fault, *Tectonophysics*, **243**, 97-118.

NIKONOV, A.A. (1995): The stratigraphic method in the study of large past earthquakes, *Quat. Int.*, **25**, 47-55.

PANTOSTI, D. and R.S. YEATS (1993): Palaeoseismology of great earthquakes of the late Holocene, *Annali di Geofisica*, **36** (3-4), 237-257.

PARRY, W.T. and R.L. BRUHN (1990): Fluid pressure transients on seismogenic normal faults. *Tectonophysics*, **179**, 335-344.

PLAFKER, G. and M. RUBIN (1967): Vertical tectonic displacements in South-Central Alaska during and prior to the great 1964 earthquake, *J. Geosci. Osaka City Univ.*, **10**, 53-66.

PETIT, J.P. (1987): Criteria for the sense of movement on fault surfaces in brittle rocks, *J. Struct. Geol.*, **9**, 597-608.

PINAR A., Y. HONKURA and M. KIKUCHI (1996): A rupture model of the 1967 Mudurnu Valley, Turkey earthquake and its implication for seismotectonics in the western part of the North Anatolian Fault, *Geophys. Res. Lett.*, **23**, 29-32.

POWER, W.L. and T.E. TULLIS (1989): The relationship between slickenside surfaces in fine-grained quartz and the seismic cycle, *J. Struct. Geol.*, **11**, 879-893.

RODGERS, D.A. (1980): Analysis of pull-apart basin development produced by en echelon strike-slip faults, in *Sedimentation in Oblique-Slip Mobile Zones*, edited by P.F. BALLACE and H.G. READING, Int. Assoc. Sed. Spec. Publ., No. 4, 27-41.

SCHWARTZ, D.P. (1987): Earthquakes of the Holocene, *Rev. Geophys.*, **25**, 1197-1202.

SCHWARTZ, D.P. and K.J. COPPERSMITH (1984): Fault behaviour and characteristic earthquakes: examples from Wasatch and San Andreas Faults, *J.Geophys. Res.*, **89**, 5681-5698.

SIBSON, R.H. (1977): Fault rocks and fault mechanisms, *J. Geol. Soc. London*, **133**, 191-213.

SIBSON, R.H. (1985): Stopping of earthquake ruptures at dilatational fault jogs, *Nature*, **316**, 248-251.

SLEMMONS, D.B. and C.M. DE POLO (1986): Evaluation of active faulting and associated hazards, in *Studies in Geophysics, Active Tectonics* edited by R.E. WALLACE, panel Chairman, 45-62.

SONDER, L.J. (1990): Effects of density contrasts on the orientation of stresses in the lithosphere: relation to principal stress directions in the Transversal Tanges, California, *Tectonics*, **9**, 761-771.

STEWART, G.S. and H. KANAMORI (1982): Complexity of rupture in large strike-slip earthquakes in Turkey, *Phys. Earth Planet. Inter.*, **28**, 70-84.

WESTERWAY, R. (1994): Deformation around stepovers in strike-slip fault zones, *J. Struct. Geol.*, **15**, 831-846.

XIAOHAN, L. (1983): Perturbations de contraintes liées aux structures cassantes dans les calcaires fins du Languedoc, Observations et simulations methématiques, Montpellier, Université des Sciences et Techniques du Languedoc, p. 130.

YOUD, T.L. and D.M. PERKINS (1987): Mapping of liquefaction severity index, *J. Geotech. Eng.*, **113**, 1374-1392.